

Favored B_c decay modes to search for a Majorana neutrinoSanjoy Mandal[†] and Nita Sinha^{*}*The Institute of Mathematical Sciences, C.I.T Campus, Tharamani, Chennai 600 113, India*

(Received 1 April 2016; published 1 August 2016)

Recently, the LHCb collaboration reported the observation of the decay mode $B_c^- \rightarrow \bar{B}_s^0 \pi^-$ with the largest exclusive branching fraction amongst the known decay modes of all the B mesons. Here we propose a search for a few lepton-number violating ($\Delta L = 2$) decay modes of B_c which can only be induced by Majorana neutrinos. Distinguishing between Dirac and Majorana nature of neutrinos is an outstanding problem and hence, all possible searches for Majorana neutrinos need to be carried out. Since the lepton number violating modes are expected to be rare, when using meson decay modes for these searches one expects CKM favored modes to be the preferred ones; $B_c \rightarrow B_s$ is one such transition. With a resonance enhancement of the Majorana neutrino mediating the $B_c^- \rightarrow \bar{B}_s^0 \ell_1^- \ell_2^- \pi^+$ modes one can hope to observe these rare modes, or, even their nonobservation can be used to obtain tight constraints on the mixing angles of the heavy Majorana singlet with the light flavour neutrinos from upper limits of the branching fractions. Using these modes we obtain exclusion curves for the mixing angles which are tighter or compatible with results from earlier studies. However, we find that the relatively suppressed mode $B_c^- \rightarrow J/\psi \ell_1^- \ell_2^- \pi^+$ can provide even tighter constraints on $|V_{eN}|^2$, $|V_{\mu N}|^2$, $|V_{eN} V_{\mu N}|$, and in a larger range of the heavy neutrino mass. Further, exclusion regions for $|V_{eN} V_{\tau N}|$, $|V_{\mu N} V_{\tau N}|$ can also be obtained for masses larger than those accessible in tau decays. Upper limits on $\mathcal{B}(B_c^- \rightarrow \pi^+ \ell_1^- \ell_2^-)$ can also result in stringent exclusion curves for all the mixing elements, including that for $|V_{\tau N}|^2$ in a mass range where it is unconstrained thus far.

DOI: 10.1103/PhysRevD.94.033001

I. INTRODUCTION

The discovery of neutrino oscillations [1–11] confirming the existence of at least two nonvanishing neutrino mass-squared differences necessitates physics beyond the standard model (SM). In principle, neutrino mass could be simply generated by addition of right-handed (RH) neutrinos through the Higgs mechanism, but to get neutrino masses less than 1 eV, the neutrino Yukawa coupling has to be extremely small $\sim \mathcal{O}(10^{-12})$. Hence alternate mechanisms for neutrino mass have been proposed. Among these the seesaw mechanism [12–17] provides a natural explanation of the smallness of neutrino mass. The simplest realization of the seesaw, the so-called type-I seesaw, requires the existence of a set of heavy electroweak singlet (sterile) lepton number violating (LNV) Majorana fermions, N . A typical scale for the Majorana mass m_N in grand unified theories (GUTs) [13] is of the order of the GUT scale, but in general, in various other scenarios, sterile neutrinos can lie in a wide range of masses. In particular, in low energy seesaw models [18,19] sterile neutrinos may have mass between ~ 100 MeV to few GeV. Sterile neutrinos have also been invoked to explain the LSND [20,21], Miniboone [22–24] and reactor [25–27] anomalies. A viable dark matter candidate is a KeV sterile neutrino [28–34]. Other astrophysical observations

including supernovae permit sterile neutrinos mixed with active ones. While cosmological/astrophysical constraints on sterile neutrinos are strong, they are model dependent and hence laboratory searches and constraints on sterile neutrinos, particularly Majorana sterile neutrinos are rather important. Sterile neutrinos have been searched for in the laboratory through peak searches in leptonic decays of pions and kaons [35]. The lepton spectrum would show a monochromatic line at a lower energy in presence of a heavy neutrino. These have provided tight constraints on the mixing angle of the sterile neutrino with the active ones. Heavy neutrinos have also been looked for through searches of their visible decay products. Searches for sterile neutrinos including majorana sterile neutrinos need to be performed at all possible scales, as their discovery may provide hints of the new physics responsible for neutrino mass generation.

One of the promising processes to explore Majorana neutrinos is through neutrinoless double beta decay which may be experimentally feasible due to the large samples of the decaying nuclei, however, on the theoretical side this involves large uncertainties coming from the nuclear matrix elements making it harder to extract information on neutrino properties. The rare LNV meson and tau decays can be more accurately evaluated [36–38] and although their decay rates may be extremely small, they may be accessible with current and future high luminosity machines. In the last decade or so, many experimental collaborations, CLEO [39–41], FOCUS [42], BABAR [43],

^{*}nita@imsc.res.in[†]smandal@imsc.res.in

BELLE and more recently LHCb [44], have searched for such LNV processes. On the theoretical and phenomenological side as well, considerable effort has been made in proposing possible modes that could probe SM singlet Majorana neutrinos in various mass ranges and constrain their mixing parameters. This includes proposals to search for heavier neutrinos at accelerator and collider experiments such as, e^+e^- [45–50], $e\gamma$ [46,51], pp and $p\bar{p}$ [46,49,50,52–57], e^-e^- [50,58], as well as in top quark and W-boson rare decays [59,60].

While various B , B_s and B_c meson decay modes have already been suggested, here we propose a few additional B_c decay modes that may perhaps be preferable for Majorana neutrino searches. The B_c mesons are unique, in being the only states consisting of two heavy quarks of different flavours ($b\bar{c}$ for B_c^-). The weak decay of the b quark will be Cabibbo suppressed, for both $b \rightarrow c$, (λ^2 suppressed) and $b \rightarrow u$ (λ^3 suppressed) transitions. However, for the $c \rightarrow s$ decay, it will be a Cabibbo favoured transition. Hence, the mode $B_c^- \rightarrow \bar{B}_s^0 \ell_1^- \ell_2^- \pi^+$ is expected to have a larger branching fraction than the other rare lepton number violating decay modes of bottom mesons considered so far. Further, for a heavy neutrino in the mass range $\sim(0.1 - 0.9)$ GeV, it is kinematically possible for it to be produced as an intermediate on mass shell state, resulting in an additional resonance enhancement of the transition rate. Note that below 0.1 GeV tight constraints already exist on $|V_{eN}|^2$ from pion decay.

The $B_c^- \rightarrow \bar{B}_s^0 \pi^-$ mode has already been observed by LHCb [61]. B_c decays to other hadronic modes have also been observed by ATLAS [62] and CMS [63], hence in addition to LHCb, ATLAS and CMS may also be able to perform the search for Majorana neutrinos via this B_c decay mode. In the proton-proton collisions at the Large Hadron Collider, B_c mesons are expected to be mainly produced through the gluon-gluon fusion process $gg \rightarrow B_c^- + \bar{b} + c$ [64]. Hence, the production cross section would be expected to increase in the 13/14 TeV run substantially. This, along with the luminosity of the order of few fb^{-1} in Run II, leads one to believe that searches for this rare LNV B_c decay modes may be feasible.

In the next section, we give the formalism for the extension of the SM to include right-handed singlets. In Sec. III, the four-body decay rate for $B_c^- \rightarrow \bar{B}_s^0 \ell_1^- \ell_2^- \pi^+$ mode is evaluated and the expected upper limits on branching ratios for these modes are used to obtain bounds on the mixings of the heavy neutrino with the light flavored ones. In Sec. IV, the modes $B_c^- \rightarrow J/\psi \ell_1^- \ell_2^- \pi^+$ and $B_c^- \rightarrow \pi^+ \ell_1^- \ell_2^-$ are discussed. We find that although these modes are not Cabibbo favored, the ease of reconstruction of the final states for these modes results in tighter possible upper limits for the branching fractions and in addition the phase space enhancement helps in obtaining tighter exclusion curves for the mixing elements. Finally in Sec. V, we conclude.

II. FORMALISM FOR HEAVY NEUTRINO MIXING

We extend the SM to include n right-handed SM singlets along with the three generation of left-handed SM $SU(2)$ doublets [36]:

$$L_{aL} = \begin{pmatrix} \nu_a \\ \ell_a \end{pmatrix}_L, \quad N_{bR},$$

where $a = 1, 2, 3$ and $b = 1, 2, 3, \dots, n$. In this model, flavor eigenstates $\nu_{\ell L}$ can be written in terms of the mass eigenstates as,

$$\nu_{\ell L} = \sum_{m=1}^3 U_{\ell m} \nu_{mL} + \sum_{m'=4}^{3+n} V_{\ell m'} N_{m'L}^c, \quad (1)$$

with $UU^\dagger + VV^\dagger = 1$.

We take a phenomenological approach regarding the mass and mixing elements of the heavy singlet neutrino, taking them to be free parameters, constrained only by experimental observations. We denote by $V_{\ell N}$ the mixing coefficient between the standard flavor neutrino ν_ℓ ($\ell = e, \mu, \tau$) and the heavy mass eigenstate N . The charged current and neutral current interactions of the leptons in the basis of mass eigenstates are given by:

$$\begin{aligned} \mathcal{L}_\ell^{CC} &= -\frac{g}{\sqrt{2}} W_\mu^+ \left(\sum_{\ell=e}^{\tau} \sum_{m=1}^3 U_{\ell m}^* \bar{\nu}_m \gamma^\mu P_L \ell \right. \\ &\quad \left. + \sum_{\ell=e}^{\tau} \sum_{m'=4}^{3+n} V_{\ell m'}^* \overline{N_{m'}^c} \gamma^\mu P_L \ell \right) + \text{H.c.}, \\ \mathcal{L}_\ell^{NC} &= -\frac{g}{2 \cos \theta_W} Z_\mu \left(\sum_{\ell=e}^{\tau} \sum_{m=1}^3 U_{\ell m}^* \bar{\nu}_m \gamma^\mu P_L \nu_\ell \right. \\ &\quad \left. + \sum_{\ell=e}^{\tau} \sum_{m'=4}^{3+n} V_{\ell m'}^* \overline{N_{m'}^c} \gamma^\mu P_L \nu_\ell \right) + \text{H.c.}, \quad (2) \end{aligned}$$

where $P_L = \frac{(1-\gamma_5)}{2}$, ψ^c is the charged conjugate, g is the $SU(2)_L$ gauge coupling. The diagonalized Majorana mass terms for the neutrinos can be written as:

$$\mathcal{L}_m^\nu = -\frac{1}{2} \left(\sum_{m=1}^3 m_m^\nu \overline{\nu}_{mL} \nu_{mR}^c + \sum_{m'=4}^{3+n} m_{m'}^N \overline{N_{m'L}^c} N_{m'R} \right) + \text{H.c.}, \quad (3)$$

III. $B_c^- \rightarrow \bar{B}_s^0 \ell_1^- \ell_2^- \pi^+$ DECAYS

A. Evaluation of the four-body decay rate

For the four-body decay $B_c^-(p) \rightarrow \bar{B}_s^0(k_1) \ell_1(k_2) \ell_2(k_3) \times \pi^+(k_4)$, where $\ell_1, \ell_2 = e, \mu$, only s-channel diagrams shown in Fig. 1 contribute. Hence, the Majorana neutrino N that induces this LNV process can appear as an intermediate on mass shell state, leading to an enhancement of

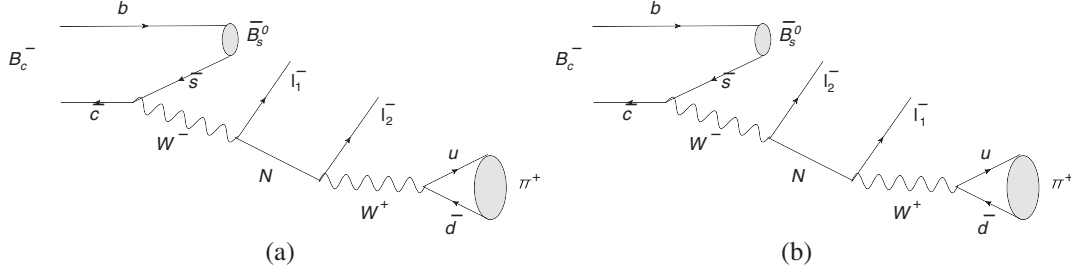


FIG. 1. (a) Feynman diagram for the decay $B_c^- \rightarrow \bar{B}_s^0 \ell_1^- \ell_2^- \pi^+$, (b) a second diagram that arises from the exchange of the two leptons.

the decay rate. Note that the second diagram [Fig. 1(b)] arises from the exchange of the two leptons. We assume that there is only one Majorana neutrino, that lies in the range, between $\sim(0.1 - 0.9)$ GeV that kinematically allows it to be on mass shell. Moreover, being much heavier than the active light neutrinos, the cosmological and LEP bounds would imply that such a neutrino would have to be necessarily an electroweak gauge singlet or sterile.

The decay amplitude for the processes depicted in Fig. 1 can be expressed as,

$$i\mathcal{M} = (\mathcal{M}_{\text{lep}})_{\beta\mu} (\mathcal{M}_{\text{had}})^{\beta\mu}, \quad (4)$$

where we can write the leptonic part as,

$$(\mathcal{M}_{\text{lep}})_{\beta\mu} = \frac{\sqrt{2}G_F V_{cs}^* V_{ud} V_{\ell_1 N} V_{\ell_2 N} m_N}{(p - k_1 - k_2)^2 - m_N^2 + im_N \Gamma_N} \times \bar{u}(k_3) \gamma_\beta \gamma_\mu P_R v(k_2) + (k_2 \leftrightarrow k_3, \ell_1 \leftrightarrow \ell_2), \quad (5)$$

where G_F is the Fermi coupling constant, $V_{\ell_i N}$ ($i = 1, 2$) are the mixing elements between the neutrino of flavor state ν_{ℓ_i} and mass eigenstate N and Γ_N is the total decay width of the heavy neutrino N , obtained by summing over all accessible final states. The hadronic tensor is a product of a transition matrix element of B_c to B_s , and a matrix element for the production of a pion:

$$(\mathcal{M}_{\text{had}})^{\beta\mu} = \frac{G_F}{\sqrt{2}} V_{cs} V_{ud} \langle \bar{B}_s^0(k_1) | \bar{s} \gamma^\mu c | B_c^-(p) \rangle \langle \pi^+(k_4) | \bar{u} \gamma^\beta d | 0 \rangle, \quad (6)$$

where V_{cs}, V_{ud} are the Cabibbo-Kobayashi-Maskawa (CKM) matrix elements. The above two hadronic matrix elements can be written as,

$$\begin{aligned} \langle \bar{B}_s^0(k_1) | \bar{s} \gamma^\mu c | B_c^-(p) \rangle &= (F_+(q^2)(p + k_1)^\mu + F_-(q^2)(p - k_1)^\mu), \\ \langle \pi^+(k_4) | \bar{u} \gamma^\beta d | 0 \rangle &= i f_\pi k_4^\beta, \end{aligned} \quad (7)$$

where $F_+(q^2), F_-(q^2)$ ($q \equiv p - k_1$) are the momentum transfer squared dependent B_c^- to \bar{B}_s^0 transition form factors and f_π is the decay constant of pion. In terms of these form factors and decay constant, we can write the amplitude \mathcal{M} as,

$$\begin{aligned} \mathcal{M} &= \frac{G_F^2 V_{cs} V_{ud} V_{\ell_1 N}^* V_{\ell_2 N} f_\pi}{(p - k_1 - k_2)^2 - m_N^2 + im_N \Gamma_N} (F_+(q^2)(p + k_1)^\mu \\ &\quad + F_-(q^2)(p - k_1)^\mu) \\ &\quad \bar{u}(k_3) \gamma_\beta \gamma_\mu (1 + \gamma_5) v(k_2) k_4^\beta + (k_2 \rightarrow k_3, \ell_1 \leftrightarrow \ell_2). \end{aligned} \quad (8)$$

The form factors for $B_c^- \rightarrow \bar{B}_s^0$ have been calculated in the framework of 3-point QCD sum rule in Ref. [65]. The q^2 dependence takes a simple pole form:

$$F_+(q^2) = \frac{F_+(0)}{1 - \frac{q^2}{M_p^2}}, \quad F_-(q^2) = \frac{F_-(0)}{1 - \frac{q^2}{M_p^2}}, \quad (9)$$

where $F_+(0) = 1.3$ and $F_-(0) = -5.8$, and $M_p = 1.7 \div 1.8$ GeV. The accuracy of the sum rules used is determined by the variation of various parameters. It is claimed in [65] that these variations result in $\frac{\delta F}{F} \approx 5\%$. To avoid this theoretical uncertainty and model dependence in the form factors, we recommend that the form factors should be determined experimentally by measurement of the semi-leptonic mode, $B_c^- \rightarrow \bar{B}_s^0 \mu^- \bar{\nu}_\mu$. Alternately, perhaps lattice estimation of the form factors may also be possible.

Although the heavy sterile neutrino N is a SM singlet, it can decay via charged current and neutral current interactions, due to its mixing with the active neutrinos as is evident from the Lagrangian (2). The total decay width Γ_N is given by:

$$\begin{aligned}
\Gamma_N = & \sum_{\ell', P^0} \Gamma^{\nu_{\ell'} P^0} + \sum_{\ell', V^0} \Gamma^{\nu_{\ell'} V^0} + \sum_{\ell', P^+} 2\Gamma^{\ell^- P^+} + \sum_{\ell', V^+} 2\Gamma^{\ell^- V^+} \\
& + \sum_{\bar{\ell}_1, \bar{\ell}_2 (\bar{\ell}_1 \neq \bar{\ell}_2)} 2\Gamma^{\bar{\ell}_1 \bar{\ell}_2 \nu_{\bar{\ell}_2}} + \sum_{\ell', \ell'_2} \Gamma^{\nu_{\ell'} \ell'_2 \ell'_2} + \sum_{\ell'} \Gamma^{\nu_{\ell'} \nu \bar{\nu}}.
\end{aligned} \tag{10}$$

In the mass range, which permits the heavy neutrino to be resonantly produced in the decay mode $B_c^- \rightarrow \bar{B}_s^0 \ell_1^- \ell_2^- \pi^+$ the leptons $\ell, \bar{\ell}_1, \bar{\ell}_2, \ell'_2$ can be e or μ , while ℓ' can be e, μ or τ , charged pseudoscalars (P^+) that can contribute are π^+ and K^+ , while π^0 and η are the contributing neutral pseudoscalars (P^0), the charged vector mesons (V^+) will include ρ^+ and K^{*+} and the neutral vector mesons (V^0) that need to be included are ρ^0 and ω .¹ The detailed expressions for the decay rates for each of these channels can be found in Refs. [36,38].

For the case of $B_c^- \rightarrow J/\psi \ell_1^- \ell_2^- \pi^+$ allowed mass range of m_N is (0.1 – 3) GeV. This will allow the additional charged pseudoscalar mesons: D^+, D_s^+ and charged vector mesons: D^{*+}, D_s^{*+} to contribute, provided ℓ is either e or μ ; for $\ell = \tau$ the mesons can only be $\pi^+, K^+, \rho^+, K^{*+}$. Additional contributing neutral pseudoscalar mesons are: η' and η_c while, ϕ and J/ψ are the heavier neutral vector mesons that can also be produced in the decays of N . $\bar{\ell}_1$ or $\bar{\ell}_2$ can now also be a τ .

For the case of $B_c^- \rightarrow \ell_1^- \ell_2^- \pi^+$ the allowed mass range in which N can be resonantly produced is (0.1 – 6) GeV. Charged pseudoscalar meson B^+ and vector meson B^{*+} will also contribute now for $\ell = e, \mu$. For $\ell = \tau$, the additional accompanying mesons will be $D^+, D_s^+, D^{*+}, D_s^{*+}$. Also, ℓ'_2 can also be τ .

We have reevaluated Γ_N using the meson masses and decay constants from Ref. [66], in the relevant mass range for the B_c decay modes considered here and write it in the form,

$$\Gamma_N = a_e(m_N)|V_{eN}|^2 + a_\mu(m_N)|V_{\mu N}|^2 + a_\tau(m_N)|V_{\tau N}|^2, \tag{11}$$

where, a_e, a_μ and a_τ are functions of the Majorana neutrino mass and hence will differ from mode to mode. In Fig. 2, we plot the decay width Γ_N as function of mass m_N , for the mixings $|V_{eN}| = |V_{\mu N}| = |V_{\tau N}| = 1$. The unitarity condition in Eq. (1) implies the following constraints on the mixing elements, $|V_{eN}|^2, |V_{\mu N}|^2$ and $|V_{\tau N}|^2$:

¹Note the V^0 cannot be K^{*0} (or any other open flavor neutral meson), as the $\nu_{\ell'} V^0$ arises from a NC interaction, K^{*0} can then only be produced via a flavor changing neutral current, which is not possible at tree level. We differ on this point from Refs. [36,38].

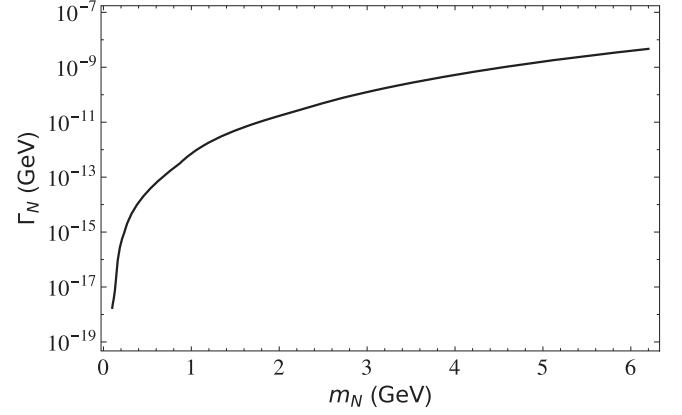


FIG. 2. Heavy neutrino decay width, Γ_N as a function of the mass m_N when the magnitude of all the mixing angles $|V_{\ell N}| = 1$ ($\ell = e, \mu, \tau$). A bigger range for m_N is chosen than that which allows a resonant enhancement of the $B_c^- \rightarrow \bar{B}_s^0 \ell_1^- \ell_2^- \pi^+$ decay, so as to include the larger values of m_N that will be permitted by the other B_c decay modes to be discussed in Sec. IV.

$$\begin{aligned}
|U_{e1}|^2 + |U_{e2}|^2 + |U_{e3}|^2 + |V_{eN}|^2 &= 1, \\
|U_{\mu1}|^2 + |U_{\mu2}|^2 + |U_{\mu3}|^2 + |V_{\mu N}|^2 &= 1, \\
|U_{\tau1}|^2 + |U_{\tau2}|^2 + |U_{\tau3}|^2 + |V_{\tau N}|^2 &= 1,
\end{aligned} \tag{12}$$

where $U_{ei}, U_{\mu i}$, and $U_{\tau i}$, $i = 1, 2, 3$ are the Pontecorvo-Maki-Nakagawa-Sakata (PMNS) matrix elements. Using the 3σ ranges of the PMNS matrix elements obtained from a global analysis of neutrino oscillation data [67], we calculate the bounds on $|V_{eN}|^2, |V_{\mu N}|^2, |V_{\tau N}|^2$ to be:

$$\begin{aligned}
|V_{eN}|^2 &\leq 0.075434, \\
|V_{\mu N}|^2 &\leq 0.377898, \\
|V_{\tau N}|^2 &\leq 0.376088.
\end{aligned} \tag{13}$$

The 3σ ranges of the PMNS matrix elements of Ref. [67] are consistent with those obtained by a study of unitarity of the neutrino mixing matrix in [68]. We wish to point out that these bounds are rather naive and are expected to serve only as a reasonable guess. Tighter bounds do exist from a combined analysis of unitarity bounds [69]. For TeV scale neutrinos constraints from LEP are even tighter [70]. Bounds from Tau, Kaon and other meson decays have also been obtained [36–38]. Our focus here will be on the bounds obtainable from some B_c decay modes. A detailed review on experimental and cosmological constraints on heavy neutrinos, is given in Ref. [71]. Figure 3 displays the heavy neutrino decay width without any assumptions, and using the maximum values for $|V_{\ell N}|^2, \ell = e, \mu, \tau$ permitted by unitarity and global fits to neutrino oscillation data. For the mass range of our interest, Γ_N is very small, $\mathcal{O}(10^{-17} - 10^{-8})$ GeV, if the mixing $|V_{eN}|^2 = |V_{\mu N}|^2 = |V_{\tau N}|^2 = 1$ and even smaller for more realistic values of

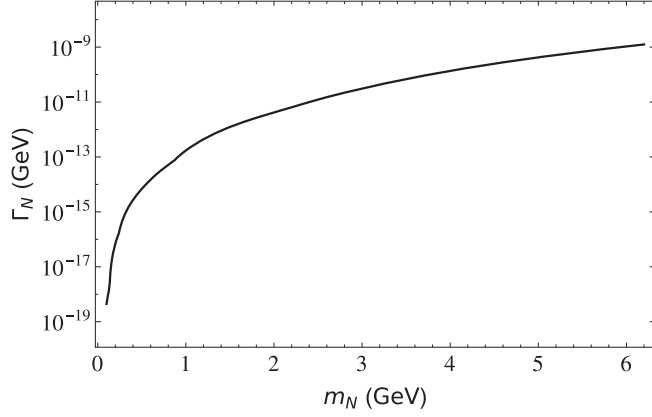


FIG. 3. Heavy neutrino decay width as a function of the mass m_N with the maximum values of the mixing angles, $|V_{\ell N}|^2$, $\ell = e, \mu, \tau$ allowed by unitarity and the global fits to oscillation data.

these mixing angles. The small width of N will imply that the heavy neutrino may travel outside the detector before decaying and the resulting decay products may not be visible. We will discuss this issue further in Sec. IV. The narrow decay width of N allows the two propagators for N , in Eq. (8) to be written as,

$$\frac{1}{(p_N^2 - m_N^2)^2 + m_N^2 \Gamma_N^2} \simeq \frac{\pi}{m_N \Gamma_N} \delta(p_N^2 - m_N^2). \quad (14)$$

Moreover, in the narrow width approximation the two channels contribute as a sum to the total decay width, as the interference term is negligible.

Most of the earlier studies of LNV meson and tau decays have focused on three-body decays. A few more recent phenomenological studies [60,72–75] of four-body LNV processes have also been performed, including an experimental search through the mode $B^- \rightarrow D^0 \pi^+ \mu^- \mu^-$ by LHCb [76]. The particular four-body B_c decay mode being considered here has the advantage of being Cabibbo favored and hence enhanced.

To calculate the four-body phase space required for evaluating the decay rate $\Gamma(B_c^-(p) \rightarrow \bar{B}_s^0(k_1) \ell_1(k_2) \ell_2 \times (k_3) \pi^+(k_4)) = \frac{1}{2m} \int d_4(ps) |\mathcal{M}|^2$, the final particles can be partitioned into two subsystems X_{12} and X_{34} , each of which subsequently decays into a two-body state. Hence, the four-body phase space integral is decomposed into a product of three two-body phase space integrals:

$$d_4(ps) = d_2(ps B_c^- \rightarrow X_{12} X_{34}) d_2(ps X_{12} \rightarrow k_1 k_2) d_2 \times (ps X_{34} \rightarrow k_3 k_4) dM_{12}^2 dM_{34}^2, \quad (15)$$

where $X_{12} = (k_1 + k_2)$, $X_{34} = (k_3 + k_4)$, $X_{12}^2 = M_{12}^2$ and $X_{34}^2 = M_{34}^2$, $p^2 = m^2$ and $k_i^2 = m_i^2$. The four-body phase space therefore takes the form,

$$d_4(ps) = \frac{1}{n!} \frac{1}{(4\pi)^6} \frac{1}{4} \lambda^{\frac{1}{2}} \left(1, \frac{M_{12}^2}{m^2}, \frac{M_{34}^2}{m^2} \right) \lambda^{\frac{1}{2}} \left(1, \frac{m_1^2}{M_{12}^2}, \frac{m_2^2}{M_{12}^2} \right) \times \lambda^{\frac{1}{2}} \left(1, \frac{m_3^2}{M_{34}^2}, \frac{m_4^2}{M_{34}^2} \right) dM_{12}^2 dM_{34}^2 d\cos\theta_{12} d\cos\theta_{34} d\phi, \quad (16)$$

where m, m_1, m_2, m_3 , and m_4 are the masses of $B_c^-, \bar{B}_s^0, \ell_1, \ell_2$ and π^+ respectively, $\lambda(x, y, z) = x^2 + y^2 + z^2 - 2xy - 2xz - 2yz$, and $n = 2$ for identical leptons in the final state, otherwise $n = 1$. $\theta_{12}(\theta_{34})$ is the angle in the $\vec{X}_{12}(\vec{X}_{34})$ rest frame between the three momentum $\vec{k}_1(\vec{k}_3)$ and the line of flight of $\vec{X}_{12}(\vec{X}_{34})$ in the B_c rest frame. The angle ϕ is the angle between the normals to the planes defined in the B_c rest frame by the $\bar{B}_s^0 \ell_1$ pair and the $\ell_2 \pi^+$ pair. This is depicted in the four-body kinematics diagram, Fig. 12 given in the Appendix. The four momenta $k_1, k_2 (k_3, k_4)$ are first evaluated in the $\vec{X}_{12}(\vec{X}_{34})$ rest frame. To finally evaluate the decay rate in the B_c rest frame, it is assumed that \vec{X}_{12} moves in the $+\hat{z}$ direction and \vec{X}_{34} in the $-\hat{z}$ direction and the resultant boosted explicit form of all the four momenta in the B_c^- rest frame are also given in the Appendix.

Alternately, rather than calculating the full 4-body kinematics to evaluate the decay rate, the narrow width approximation can be used to evaluate the decay rate as a product of a 3-body decay rate and the branching ratio for decay of N to a 2-body mode, as specified below:

$$\Gamma(B_c^- \rightarrow \bar{B}_s^0 \ell_1^- \ell_2^- \pi^+) \approx \Gamma(B_c^- \rightarrow \bar{B}_s^0 \ell_1^- N) \cdot \frac{\Gamma(N \rightarrow \ell_2^- \pi^+)}{\Gamma_N}. \quad (17)$$

In Fig. 4, we show the curves corresponding to $\frac{\mathcal{B}(B_c^- \rightarrow \bar{B}_s^0 e^- e^- \pi^+)}{|V_{eN}|^2} / \frac{\mathcal{B}(B_c^- \rightarrow \bar{B}_s^0 e^- e^- \pi^+)}{|V_{eN}|^4}$ and $\frac{\mathcal{B}(B_c^- \rightarrow \bar{B}_s^0 \mu^- \mu^- \pi^+)}{|V_{\mu N}|^2} / \frac{\mathcal{B}(B_c^- \rightarrow \bar{B}_s^0 \mu^- \mu^- \pi^+)}{|V_{\mu N}|^4}$, as a function of the heavy neutrino mass, m_N . The regions below the curves are theoretically allowed. For this calculation, Γ_N is evaluated, either under the assumption that has been frequently used in the literature [36,38], $|V_{eN}| \sim |V_{\mu N}| \sim |V_{\tau N}|$, shown in the left figure (a) or, using the upper limits of the mixing elements, obtained in Eq. (13), leading to the maximum value of Γ_N permitted by unitarity and global fits to oscillation data, displayed in the right figure (b). Note that the few kinks in the plots in Figs. (2–4) arise from threshold for a new channel contributing to Γ_N at the corresponding m_N value (e.g. around 0.135 GeV and 0.245 GeV the visible kinks are from the threshold for $\nu \pi^0$ and $\pi^+ \mu^-$ respectively).

B. Bounds on mixing angles using upper limits on the branching ratios for $B_c^- \rightarrow \bar{B}_s^0 \ell_1^- \ell_2^- \pi^+$ decays

Using the matrix element in Eq. (8) and the narrow width approximation, Eq. (14) the LNV branching ratios can be written as:

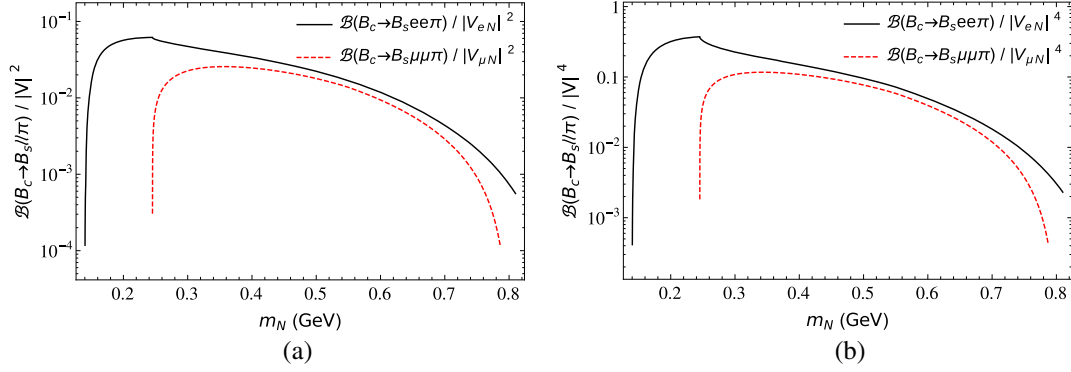


FIG. 4. (a) $\frac{\mathcal{B}(B_c^- \rightarrow \bar{B}_s^0 \ell^- \ell^- \pi^+)}{|V_{\ell N}|^2}$, where, $\ell = e, \mu$. The theoretical calculation uses Γ_N obtained with the assumption $|V_{eN}| \sim |V_{\mu N}| \sim |V_{\tau N}|$. (b) $\frac{\mathcal{B}(B_c^- \rightarrow \bar{B}_s^0 \ell^- \ell^- \pi^+)}{|V_{\ell N}|^4}$, $\ell = e, \mu$. Γ_N is obtained using the upper limits of the mixing elements allowed by unitarity and global fits to oscillation data.

$$\begin{aligned} \mathcal{B}(B_c^- \rightarrow \bar{B}_s^0 e^- e^- \pi^+) &= G_{ee}(m_N) \frac{|V_{eN}|^4}{\Gamma_N}, \\ \mathcal{B}(B_c^- \rightarrow \bar{B}_s^0 \mu^- \mu^- \pi^+) &= G_{\mu\mu}(m_N) \frac{|V_{\mu N}|^4}{\Gamma_N}, \end{aligned} \quad (18)$$

where, G_{ee} and $G_{\mu\mu}$ are functions of the Majorana mass and depend on the explicit matrix element and phase space for each of the processes. When both the like sign dileptons in Fig. 1 are not of the same flavor, then the process is not only lepton number violating but also lepton flavor violating. If the two vertices of N production and decay can be separated, then the two processes, $B_c^- \rightarrow \bar{B}_s^0 e^- N$ followed by $N \rightarrow \mu^- \pi^+$ and $B_c^- \rightarrow \bar{B}_s^0 \mu^- N$ followed by $N \rightarrow e^- \pi^+$ can be distinguished. Assuming this separation, we may write:

$$\begin{aligned} \mathcal{B}(B_c^- \rightarrow \bar{B}_s^0 e^- \mu^- \pi^+) &= G_{e\mu}(m_N) \frac{|V_{eN}|^2 |V_{\mu N}|^2}{\Gamma_N}, \\ \mathcal{B}(B_c^- \rightarrow \bar{B}_s^0 \mu^- e^- \pi^+) &= G_{\mu e}(m_N) \frac{|V_{eN}|^2 |V_{\mu N}|^2}{\Gamma_N}, \end{aligned} \quad (19)$$

where, we use the notation that the first lepton is produced along with the N , while the second lepton is produced in the decay of N ; $G_{e\mu}$ ($G_{\mu e}$) are again functions of the Majorana mass and vary with the explicit matrix element and phase space for each of the processes. Now, defining,

$$\begin{aligned} F_{ee} &\equiv \frac{\mathcal{B}^{\text{exp}}(B_c^- \rightarrow \bar{B}_s^0 e^- e^- \pi^+)}{G_{ee}(m_N)}, \\ F_{\mu\mu} &\equiv \frac{\mathcal{B}^{\text{exp}}(B_c^- \rightarrow \bar{B}_s^0 \mu^- \mu^- \pi^+)}{G_{\mu\mu}(m_N)}, \\ F_{e\mu} &\equiv \frac{\mathcal{B}^{\text{exp}}(B_c^- \rightarrow \bar{B}_s^0 e^- \mu^- \pi^+)}{G_{e\mu}(m_N)}, \\ F_{\mu e} &\equiv \frac{\mathcal{B}^{\text{exp}}(B_c^- \rightarrow \bar{B}_s^0 \mu^- e^- \pi^+)}{G_{\mu e}(m_N)}, \end{aligned} \quad (20)$$

where \mathcal{B}^{exp} are the expected experimental upper limits of the branching ratios, we can obtain the constraints:

$$\begin{aligned} \frac{|V_{eN}|^4}{\Gamma_N} &< F_{ee}, & \frac{|V_{\mu N}|^4}{\Gamma_N} &< F_{\mu\mu}, \\ \frac{|V_{eN}|^2 |V_{\mu N}|^2}{\Gamma_N} &< F_{e\mu}/F_{\mu e}. \end{aligned} \quad (21)$$

The upper limits on the \mathcal{B}^{exp} in Eq. (21) can be very simply translated into the upper limits on, $|V_{eN}|^2$, $|V_{\mu N}|^2$, $|V_{eN} V_{\mu N}|$ under the assumption, $|V_{eN}| \sim |V_{\mu N}| \sim |V_{\tau N}|$ in Γ_N . This leads Eq. (21) to result in the constraints,

$$\begin{aligned} |V_{eN}|^2 &< F_{ee}(a_e + a_\mu + a_\tau); \\ |V_{\mu N}|^2 &< F_{\mu\mu}(a_e + a_\mu + a_\tau); \\ |V_{eN} V_{\mu N}| &< F_{e\mu}/F_{\mu e}(a_e + a_\mu + a_\tau). \end{aligned} \quad (22)$$

According to Ref. [77] at the LHC with $\sqrt{s} = 14$ TeV, the beam luminosity and production cross section will be high enough that the rate of producing B_c events can be $10^8 - 10^9$ per year. A crude estimate [78] using the measured [79] ratio of production cross section times branching fractions between the $B_c^+ \rightarrow J/\psi \pi^+$ and $B^+ \rightarrow J/\psi K^+$ decays at $\sqrt{s} = 8$ TeV, indicates $\sim \mathcal{O}(10^9 - 10^{10}) B_c$ events with 10 fb^{-1} luminosity at 13/14 TeV. Ultimately, the production cross section will be directly measured by LHCb at $\sqrt{s} = 13/14$ TeV and will be known more precisely. In any case the large number of B_c events will make a search for the proposed rare LNV B_c decays feasible. Even if these decay modes are not seen, one may naively estimate that it may be possible to set upper limits on the branching ratios of $\sim \mathcal{O}(10^{-7} - 10^{-9})$. However, since the final B_s meson needs to be reconstructed via its prominent decay modes, either $B_s \rightarrow J/\psi(\mu\mu)\phi(KK)$ or $B_s \rightarrow D_s(KK\pi)\pi$, with $\mathcal{B}(B_s \rightarrow J/\psi\phi) \times \mathcal{B}(J/\psi \rightarrow \mu\mu) \times \mathcal{B}(\phi \rightarrow KK) \sim \mathcal{O}(10^{-5})$; $\mathcal{B}(B_s \rightarrow D_s\pi) \times \mathcal{B}(D_s \rightarrow KK\pi) \sim \mathcal{O}(10^{-4})$, upper limits on $\mathcal{B}(B_c^- \rightarrow \bar{B}_s^0 \ell_1^- \ell_2^- \pi^+)$ of only $\sim \mathcal{O}(10^{-5} - 10^{-4})$ may be feasible. These limits are just indicative, exact realistic limits will only be determined by the experimental collaboration, after incorporating the detection, reconstruction

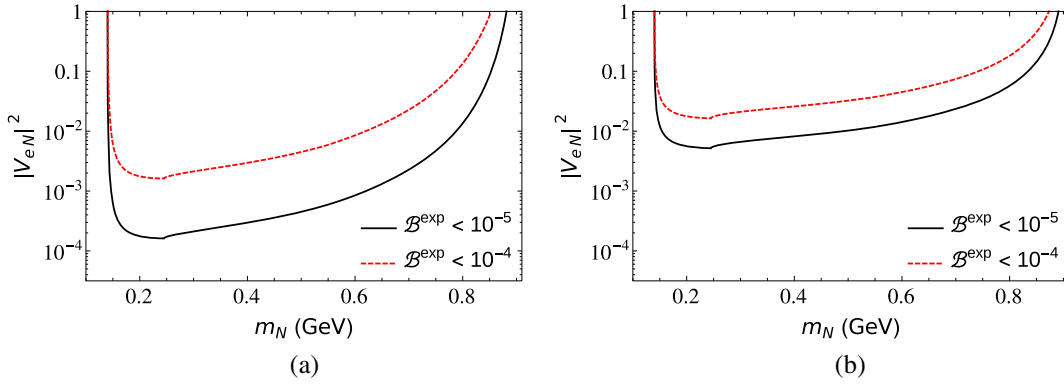


FIG. 5. Exclusion curves for the mixing element $|V_{eN}|^2$ corresponding to the different expected upper limits for branching ratio of the decay mode $B_c^- \rightarrow \bar{B}_s^0 e^- e^- \pi^+$. In Γ_N , the left figure(a) uses the assumption, $|V_{eN}| \sim |V_{\mu N}| \sim |V_{\tau N}|$, while the right figure(b) uses the maximum allowed magnitude of the mixing elements V_{eN} , $V_{\mu N}$, $V_{\tau N}$ from unitarity and the global fits to oscillation data.

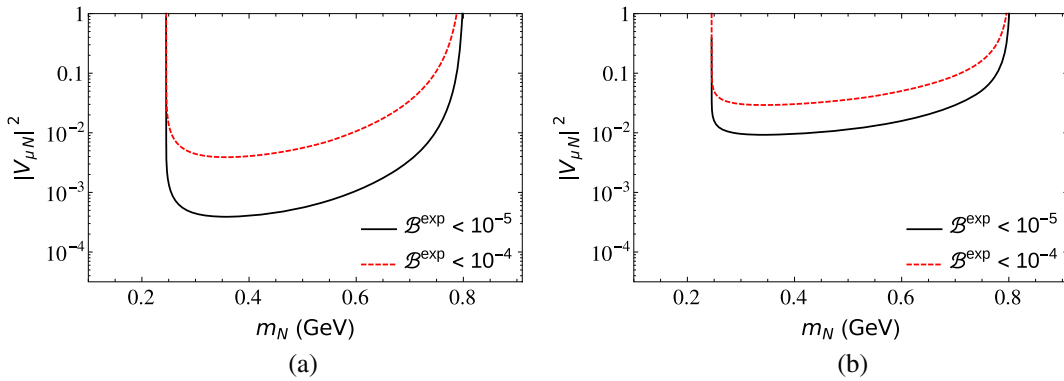


FIG. 6. Exclusion curves for the mixing element $|V_{\mu N}|^2$ from the expected upper limits for the branching fraction of the decay mode $B_c^- \rightarrow \bar{B}_s^0 \mu^- \mu^- \pi^+$. Both the left figure (a) and the right figure (b) use the same assumption/constraints for the magnitude of the mixing elements as those in Fig. 5.

efficiencies of all the final particles. Of course, tighter limits would be possible at future colliders.

In the left panels of the Figs. 5, 6 and 7, we show the exclusion curves corresponding to the constraints on the mixing angles $|V_{eN}|^2$, $|V_{\mu N}|^2$, $|V_{eN}V_{\mu N}|$ given in Eq. (22), for possible upper limits on the \mathcal{B}^{exp} ($B_c^- \rightarrow \bar{B}_s^0 \ell_1^- \ell_2^- \pi^+$), of 10^{-4} and 10^{-5} . Rather loose constraints are obtained if no assumptions regarding the mixing elements $|V_{\ell N}|^2$, $\ell = e, \mu, \tau$ are made and if the maximum values of these mixing elements permitted by unitarity and global fits to oscillation data [obtained in Eq. (13)] are used in Γ_N evaluation. This results in the upper limits on the mixing elements displayed in the right panels of the Figs. 5, 6 and 7, again if upper limits on the \mathcal{B}^{exp} ($B_c^- \rightarrow \bar{B}_s^0 \ell_1^- \ell_2^- \pi^+$) of 10^{-4} , 10^{-5} are experimentally attained.

For the lepton flavor violating case, $\ell_1 \neq \ell_2$, the mass difference of e and μ results in a slight difference in the mass range allowed for N (for its resonant production) for the two cases: when the electron is produced along with the Majorana neutrino N , while muon arises from the decay of N , or vice versa. Hence, in Fig. 7 we present the exclusion curves for these two cases separately. If the separation of

the vertices is not easily feasible, one can just add the results of the two cases in the overlapping kinematic range. Using the upper limit on the branching fractions, \mathcal{B}^{exp} ($B_c^- \rightarrow \bar{B}_s^0 \ell_1^- \ell_2^- \pi^+$) $\sim 10^{-5}$, the bounds on the mixing angles obtained for $\sim (0.1 < m_N < 0.9)$ GeV, are slightly tighter than those from other heavy meson decays considered in [36,38]. Only the constraints from K meson visible 3-body decays are tighter, but for the mass range of $\sim 0.35 < m_N < 0.90$ GeV, our exclusion limits are either tighter or compatible with the earlier constraints. A comparison of our exclusion plots against that shown in a recent analysis on global constraints on a heavy neutrino [80], again shows that these bounds could provide very tight constraints in a small range of m_N , beyond that excluded only by peak searches in K meson decays, which is otherwise so far unconstrained.²

The reasons for this improved sensitivity are that the meson decay modes considered in the literature so far have

²We wish to point out that our constraints cannot be directly compared with that in Ref. [80], as their conservative constraints are independent of the heavy neutrino decay products.

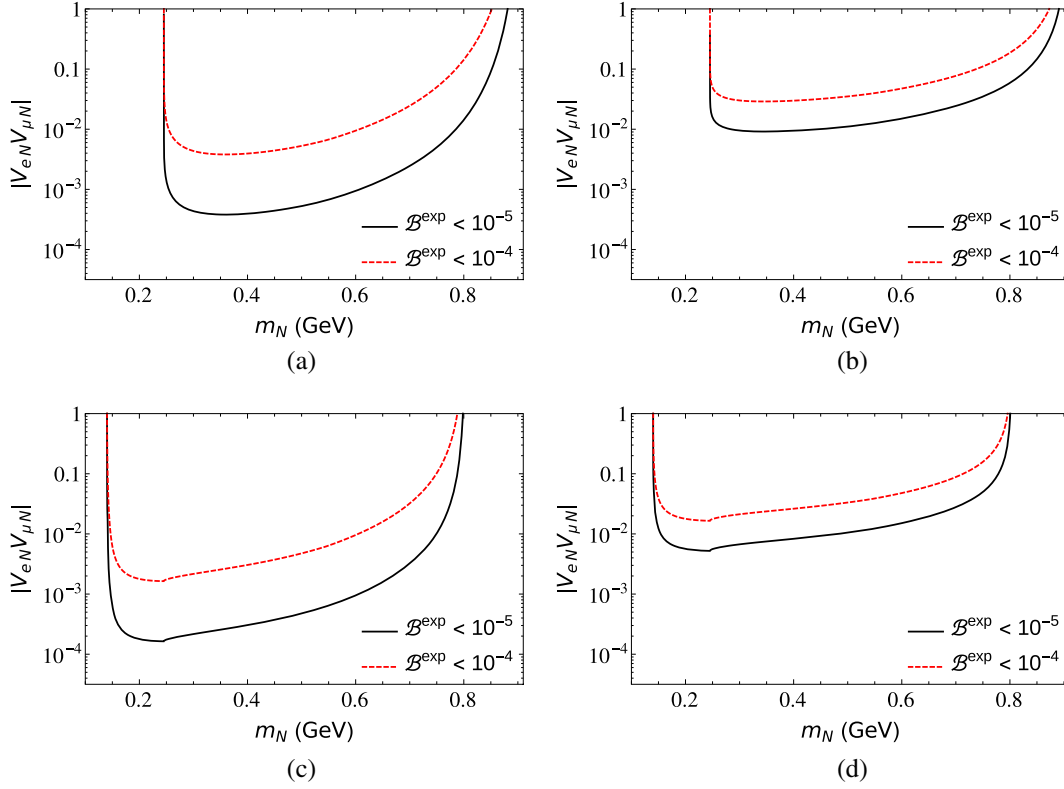


FIG. 7. Exclusion curves for the mixing element $|V_{\ell_1 N} V_{\ell_2 N}|$ from the possible upper limits for the branching fraction of the decay mode $B_c^- \rightarrow \bar{B}_s^0 \ell_1^- \ell_2^- \pi^+$, (a) is for $\ell_1 = e$ and $\ell_2 = \mu$ and uses the assumption of equal magnitudes of all the mixing elements for Γ_N , (b) is also for $\ell_1 = e$ and $\ell_2 = \mu$, but for Γ_N uses the maximum values of the mixing elements permissible by the unitarity constraints and global fits to oscillation data, (c) and (d) are for $\ell_1 = \mu$ and $\ell_2 = e$ and for Γ_N use the same assumptions as that used in figures (a) and (b) respectively.

been mostly 3-body decay modes involving the annihilation of the initial meson and the weak annihilation vertex of all heavy mesons (except D_s) suffers from Cabibbo suppression. This reduces the coefficient of the mixing elements in the decay rates, resulting in looser constraints. Hence, in spite of the mild phase space suppression this 4-body mode can result in improved exclusion limits for the mixing angles of the heavy Majorana neutrino with the light flavor neutrinos. With a larger sample of B_c events, possible at future high energy colliders, much stronger upper limits on the branching ratios would be possible, which would result in more stringent constraints on the mixing elements.

IV. OTHER B_c DECAY MODES

Although the modes $B_c^- \rightarrow \bar{B}_s^0 \ell_1^- \ell_2^- \pi^+$, are expected to have a larger branching ratios due to the Cabibbo enhancement, however, as pointed out in the last section, the reconstruction of the \bar{B}_s^0 results in a penalty of $\sim \mathcal{O}(10^{-4})$, implying that with the limited number B_c events at LHCb even in the 13/14 TeV run, upper limits on the branching ratios for these modes, smaller than 10^{-5} may not be feasible. In fact, for the modes $B_c^- \rightarrow J/\psi \ell_1^- \ell_2^- \pi^+$ which are Cabibbo suppressed, but where the reconstruction of

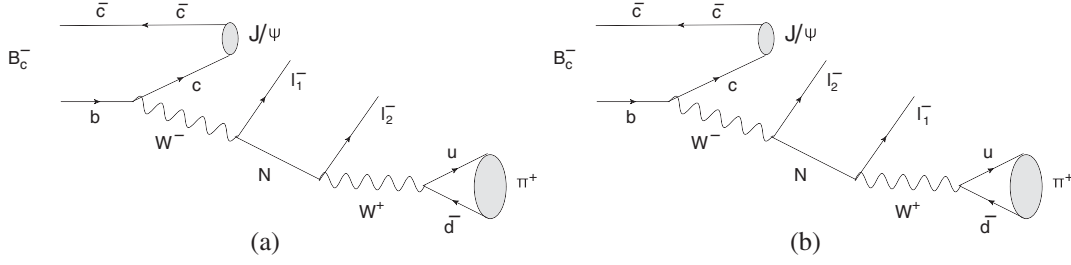
J/ψ only results in a suppression factor of $\sim \mathcal{O}(10^{-2})$, tighter upper limits on the branching fraction $\sim \mathcal{O}(10^{-7})$ may be achievable, provided the final leptons are electrons or muons. If one of the final leptons is a tau, the upper limit may be less tighter $\sim \mathcal{O}(10^{-6})$. Also, while LHCb has already searched for Majorana neutrinos via the mode $B^- \rightarrow \pi^+ \mu^- \mu^-$, perhaps a search through the mode $B_c^- \rightarrow \pi^+ \mu^- \mu^-$ may provide tighter constraints on the mixing angles.

A. $B_c^- \rightarrow J/\psi \ell_1^- \ell_2^- \pi^+$

The diagrams contributing to this decay mode are shown in Fig. 8. The leptonic tensor in the amplitude will have the same form as that in Eq. (5), while the hadronic tensor can be written as:

$$(\mathcal{M}_{\text{had}})^{\beta\mu} = \frac{G_F}{\sqrt{2}} V_{cb} V_{ud} \langle J/\psi(k_1) | \bar{b} \gamma^\mu (1 - \gamma_5) c | B_c^-(p) \rangle \times \langle \pi^+(k_4) | \bar{u} \gamma^\beta d | 0 \rangle, \quad (23)$$

Here, the hadronic matrix element of the weak current in the $B_c^- \rightarrow J/\psi$ transition in terms of the vector and axial-vector form factors is given by,


 FIG. 8. (a) Feynman diagram for the decay $B_c^- \rightarrow J/\psi \ell_1^- \ell_2^- \pi^+$, (b) diagram with the two leptons exchanged.

$$\begin{aligned} & \langle J/\psi(k_1) | \mathcal{J}^\mu | B_c^-(p) \rangle \\ & = (-F_V \epsilon^{\mu\nu\alpha\beta} \epsilon_\nu^* Q_\alpha q_\beta + iF_0^A \epsilon^{*\mu} \\ & \quad + iF_+^A (\epsilon^* \cdot p) Q^\mu + iF_-^A (\epsilon^* \cdot p) q^\mu), \end{aligned} \quad (24)$$

where, $Q = p + k_1$, $q = p - k_1$, and ϵ is the polarization vector of the J/ψ meson. The form factors, F_V, F_0^A, F_+^A and F_-^A have been estimated using QCD sum rules in Ref. [65], with the values from zero recoil evolved with the pole dependence:

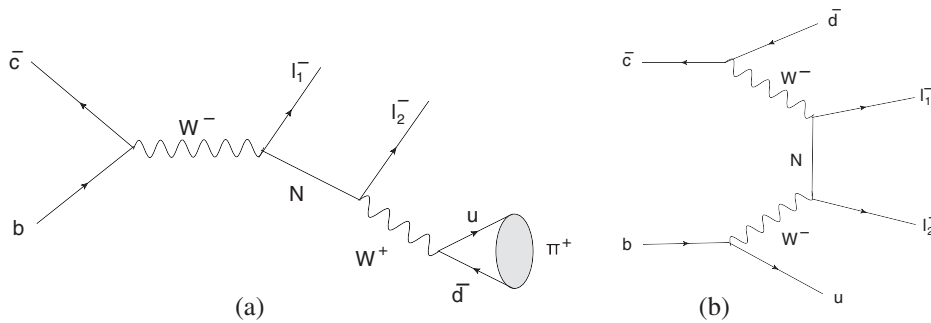
$$F_i(q^2) = \frac{F_i(0)}{1 - \frac{q^2}{M_{i,\text{pole}}^2}}, \quad (25)$$

with the numerical values: $F_V(0) = 0.11 \text{ GeV}^{-1}$, $F_0^A = 5.9 \text{ GeV}$, $F_+^A = -0.074 \text{ GeV}^{-1}$ and $F_-^A = 0.12 \text{ GeV}^{-1}$; while the pole mass used in each of the vector/axial-vector form factors for $B_c \rightarrow \bar{c}c$ is 4.5 GeV. We evaluate the four-body decay rate for this mode using the procedure analogous to that followed for the $B_c^- \rightarrow \bar{B}_s^0 \ell_1^- \ell_2^- \pi^+$ decay mode, i.e., using the narrow width approximation for N and the phase space given in Eq. (16). Of course, due to the presence of larger number of form factors, the matrix element mod-squared appears more complicated. The bounds on the mixing elements are also derived in a similar fashion, using constraints similar to that given in Eq. (22), with the corresponding parameters appropriately defined in terms of the theoretical branching fractions and the experimental upper limits for the $B_c^- \rightarrow J/\psi \ell_1^- \ell_2^- \pi^+$

mode. Note however, that the mass difference between that of B_c and J/ψ will allow neutrino masses up to over 3 GeV to be on shell. This not only allows us to constrain $|V_{eN}|^2$, $|V_{\mu N}|^2$ and $|V_{eN}V_{\mu N}|$ over a bigger mass range, but exclusion curves for $|V_{eN}V_{\tau N}|$, $|V_{\mu N}V_{\tau N}|$ can also be provided for heavy neutrino masses beyond the region probed via tau decays.

B. $B_c^- \rightarrow \pi^+ \ell_1^- \ell_2^-$

While the number of B_c events at LHCb are expected to be smaller than the number of B^\pm events, still this mode being less suppressed with respect to $B^- \rightarrow \pi^+ \ell_1^- \ell_2^-$ could possibly result in tighter constraints on the mixing angles. The diagrams contributing to this process are shown in Figs. 9. Apart from the s-channel diagram (a), there is also a t-channel diagram, where the off-shell heavy neutrino contributes. However, since this diagram is highly suppressed due to CKM suppression, as well as due to absence of resonant enhancement, we only include the dominant contribution of Fig. 9(a) (including that for the two leptons exchanged). The large mass difference between that of B_c and π meson allows both final leptons to be taus also. With only pion and electrons/muons as the final state particles, this mode should be easy to reconstruct, however, for the case of one or both of the leptons being a tau, the reconstruction will involve accounting for the tau branching fraction to the final state through which it is seen. The even wider range allowed for the heavy neutrino mass, also allows upper limit on $|V_{\tau N}|^2$, which is unconstrained by any of the τ or other meson decays.


 FIG. 9. (a) The s-channel feynman diagram for the decay $B_c^- \rightarrow J/\psi \ell_1^- \ell_2^- \pi^+$. (b) The t-channel diagram for the same process.

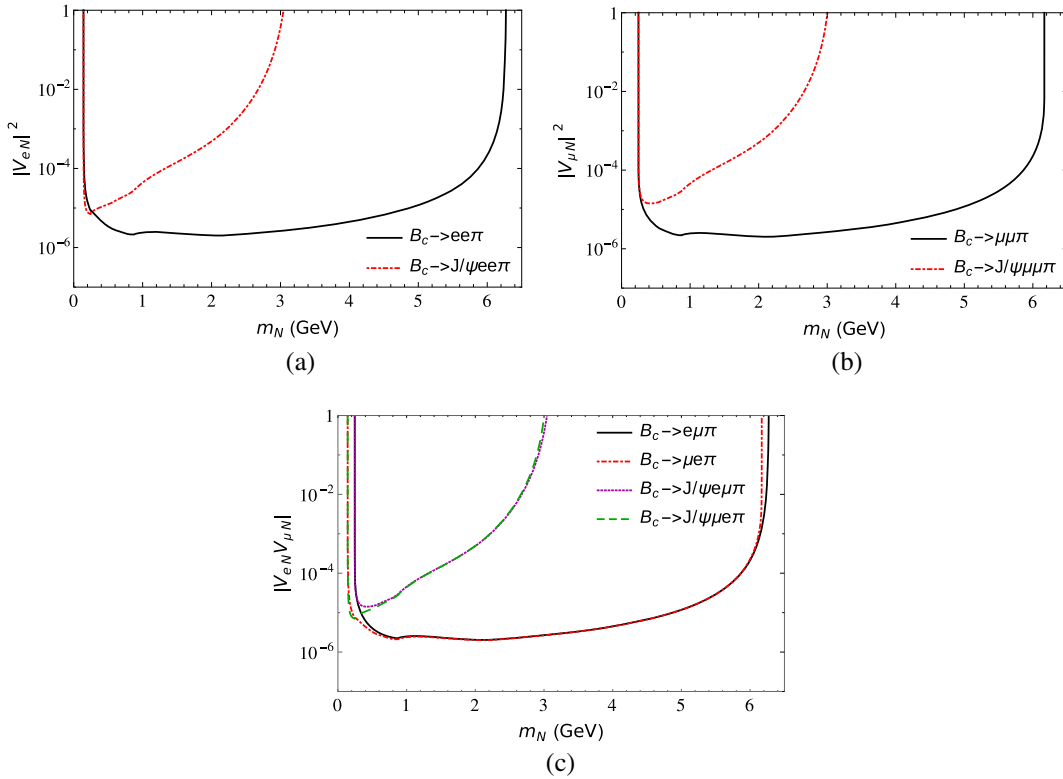


FIG. 10. Exclusion curves for the mixing element $|V_{\ell_1 N} V_{\ell_2 N}|$ from upper limits for the branching fraction $\mathcal{B}(B_c^- \rightarrow J/\psi \ell_1^- \ell_2^- \pi^+) \sim 10^{-7}$ and $\mathcal{B}(B_c^- \rightarrow \pi^+ \ell_1^- \ell_2^-) \sim 10^{-9}$. Notation regarding the ordering of the leptons is the same as that described in Sec. III. In figure (a), $l_1 = l_2 = e$, in (b) $l_1 = l_2 = \mu$ while in (c) $l_1 = e$, $l_2 = \mu$

In Fig. 10(a)–10(c) we show the exclusion curves for $|V_{eN}|^2$, $|V_{\mu N}|^2$ and $|V_{eN} V_{\mu N}|$ respectively, obtained from the expected upper limits of $\mathcal{B}(B_c^- \rightarrow J/\psi \ell_1^- \ell_2^- \pi^+) \sim 10^{-7}$ and $\mathcal{B}(B_c^- \rightarrow \pi^+ \ell_1^- \ell_2^-) \sim 10^{-9}$ ($\ell_1, \ell_2 = e$ or μ), at LHCb with $\sim 10^{10}$ B_c events. If one or both of the leptons is a tau, then its reconstruction would lead to looser upper limits on the branching fraction. Figure 11(a) shows the exclusion curves for $|V_{eN} V_{\tau N}|$, while that for $|V_{\mu N} V_{\tau N}|$ are displayed in Fig. 11(b), corresponding to the upper limits: $\mathcal{B}(B_c^- \rightarrow J/\psi \ell_1^- \ell_2^- \pi^+) \sim 10^{-6}$ and $\mathcal{B}(B_c^- \rightarrow \ell_1^- \ell_2^- \pi^+) \sim 10^{-8}$ when, ℓ_1^- or ℓ_2^- is a τ^- . Figure 11(c) shows the exclusion curve for $|V_{\tau N}|^2$ corresponding to an upper limit of $\mathcal{B}(B_c^- \rightarrow \pi^+ \tau^- \tau^-) \sim 10^{-7}$

Note that $|V_{\tau N}|^2$ is very loosely constrained, with some limits from CHARM [81,82], NOMAD [83] and DELPHI [84] collaborations, but with the mass range of $\sim (0.3 - 5.0)$ GeV almost unconstrained.³ The $B_c^- \rightarrow \pi^+ \tau^- \tau^-$ mode partially fills up this gap in providing exclusion limits in part of this range.

³Reference [85] suggests that the large data sets of the B factories may be able to place stringent limits for $100 \text{ MeV} \leq M_N \leq 1.2 \text{ GeV}$.

In each of the above studies the Majorana sterile neutrino produced in the B_c decay is assumed to propagate as a real particle and then decay after a certain distance from the production point. In the exclusion limits obtained on the mixing elements above, we assumed an idealized detector, where this distance lies within the detector length and hence the probability of this production and decay of the heavy neutrino within the detector is unity. In practice one may need to introduce a more realistic probability factor, which could possibly weaken the constraints on the mixing elements. Estimation of this effect will depend on the specific experimental set up, the momenta carried by the heavy neutrino which would depend on that of the decaying B_c meson etc. Hence this can be properly incorporated only by the respective experimental collaborations in their data analysis. In fact, LHCb has indeed accounted for this in their analysis of a few LNV B decay modes, for a Majorana neutrino of mass of 2–3 GeV [76]. However, for the case of B_c decaying at rest, in order to obtain a decay length of the heavy neutrino of about $10m$ (expected detector length), corresponding to the bounds obtained on the mixing element, $|V_{eN}|^2$ of $\sim \mathcal{O}(10^{-4}, 10^{-5}, 10^{-6})$ for the modes $B_c^- \rightarrow \bar{B}_s^0 \ell_1^- \ell_2^- \pi^+$, $B_c^- \rightarrow J/\psi \ell_1^- \ell_2^- \pi^+$ and $B_c^- \rightarrow \pi^+ \ell_1^- \ell_2^-$ respectively, the mass of N should be above 0.6, 1.4 and 2.2 GeV.

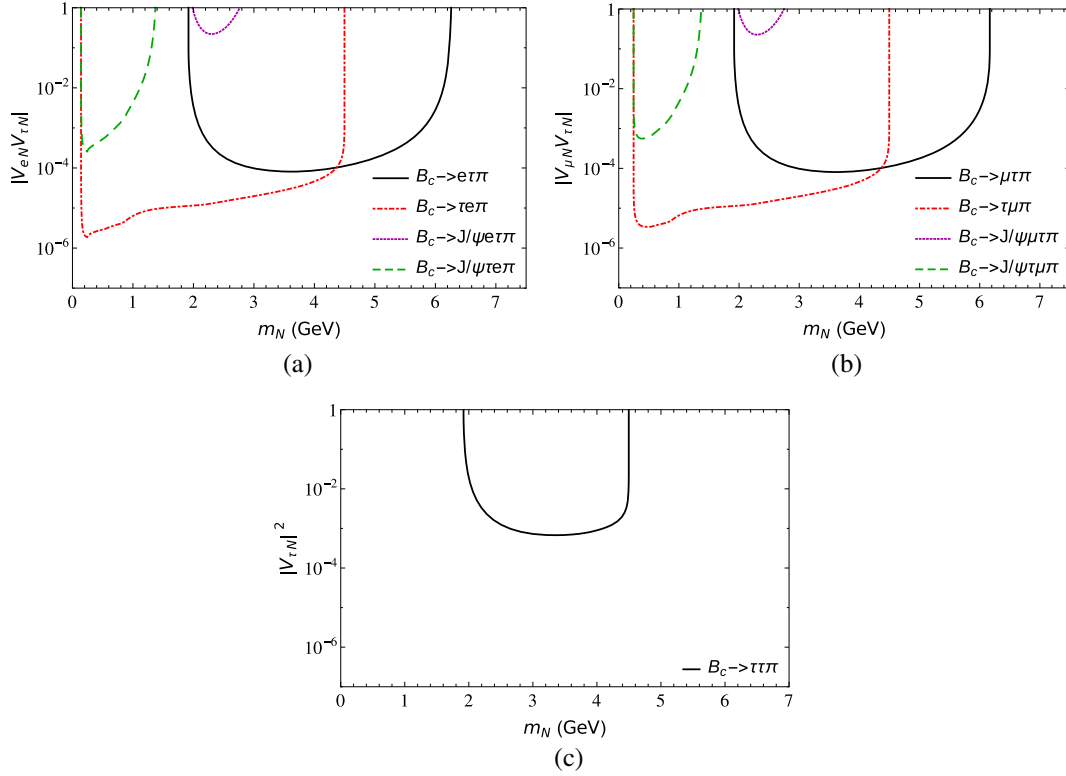


FIG. 11. Exclusion curves for the mixing element $|V_{\ell_1 N} V_{\ell_2 N}|$. For (a), one of the leptons is an electron while the second one is a tau; the upper limits used are: $\mathcal{B}(B_c^- \rightarrow J/\psi \ell_1^- \ell_2^- \pi^+) \sim 10^{-6}$, $\mathcal{B}(B_c^- \rightarrow \pi^+ \ell_1^- \ell_2^-) \sim 10^{-8}$, (b) corresponds to the case of one muon and one tau, again using the upper limits: $\mathcal{B}(B_c^- \rightarrow J/\psi \ell_1^- \ell_2^- \pi^+) \sim 10^{-6}$, $\mathcal{B}(B_c^- \rightarrow \pi^+ \ell_1^- \ell_2^-) \sim 10^{-8}$ and for (c), both final leptons are taus and the expected upper limit for $\mathcal{B}(B_c^- \rightarrow \pi^+ \ell_1^- \ell_2^-) \sim 10^{-7}$.

V. CONCLUSIONS

We propose several B_c decay modes for Majorana neutrino searches. The B_c meson is unique in being the only meson with two heavy quarks of different flavor, allowing weak decays not only of the b quark but also the c quark. The b quark decays are always Cabibbo suppressed, with λ^2 or λ^3 suppression for $b \rightarrow c$ or $b \rightarrow u$ transitions respectively. The charm quark decay on the other hand can be Cabibbo favored. Hence the amplitude for $B_c^- \rightarrow \bar{B}_s^0 \ell_1^- \ell_2^- \pi^+$, ($\ell_1, \ell_2 = e, \mu$) decays can be enhanced. These four-body decay modes involve transition form factors rather than decay constants that appear in case of annihilation of the decaying meson, as is the case for the 3-body meson decays extensively studied for Majorana neutrino searches in the literature. To avoid model dependence and theoretical uncertainties, we suggest that these form factors be measured using the semi-leptonic mode, $B_c^- \rightarrow \bar{B}_s^0 \mu^- \bar{\nu}$. For a Majorana neutrino that lies in the mass range that allows it to be on the mass shell, there is also a resonant enhancement of the process. A search for Majorana neutrinos via these rare modes which are expected to have larger branching fractions, appears more feasible. Even a nonobservation can result in

exclusion curves for the mixing angles of the heavy Majorana singlet with the flavor eigenstates, corresponding to possible upper limits for the branching fractions. These constraints are mostly tighter than those obtained from other heavy meson decay modes in earlier studies and the mass range probed lies beyond the range with stringent constraints from experimental bounds on three-body Kaon LNV decays.

In spite of the Cabibbo enhancement for the $B_c^- \rightarrow \bar{B}_s^0 \ell_1^- \ell_2^- \pi^+$ modes, the reconstruction of the B_s leads one to expect less stringent upper limits for these modes compared to that for $B_c^- \rightarrow J/\psi \ell_1^- \ell_2^- \pi^+$ modes where the J/ψ can be reconstructed more easily via the $\mu^+ \mu^-$ mode. Similarly the reconstruction of the $B_c^- \rightarrow \pi^+ \ell_1^- \ell_2^-$ mode would be less demanding. This along with the phase space enhancement of the latter two modes may result in much tighter (by almost an order of magnitude) exclusion curves for the mixing elements, $|V_{eN}|^2$, $|V_{\mu N}|^2$, $|V_{eN} V_{\mu N}|$. Further, for $|V_{eN} V_{\tau N}|$, $|V_{\mu N} V_{\tau N}|$, on which bounds exist only from tau decays, exclusion curves for masses up to about 6 GeV can be provided. Also, upper limits for $|V_{\tau N}|^2$ can be obtained in the mass range (0.3 – 5.0) GeV, where it is so far unconstrained.

ACKNOWLEDGMENTS

N. S. thanks Vanya Belyaev for communication regarding the expected B_c production cross-section at LHCb in the 13/14 TeV run. The authors thank Patrick Koppenburg for his valuable inputs and suggestions and appreciate comments from Andrew Kobach, G. López Castro, V. V. Kiselev, Sandip Pakvasa and N. G. Deshpande.

APPENDIX: FOUR-BODY KINEMATICS

To describe the kinematics of four-body decays, five independent variables are required. We choose the independent variables to be, M_{12}^2 , M_{34}^2 , θ_{12} , θ_{34} and ϕ , which for the processes, $B_c^-(p) \rightarrow \bar{B}_s^0(k_1)\ell_1^-(k_2)\ell_2^-(k_3)\pi^+(k_4)$ or $B_c^-(p) \rightarrow J/\psi(k_1)\ell_1^-(k_2)\ell_2^-(k_3)\pi^+(k_4)$ are defined as:

$$\begin{aligned} M_{12}^2 &= (k_1 + k_2)^2; & M_{34}^2 &= (k_3 + k_4)^2; \\ \cos\theta_{12} &= \frac{\hat{v} \cdot \vec{k}_1}{|\vec{k}_1|}; & \cos\theta_{34} &= \frac{-\hat{v} \cdot \vec{k}_3}{|\vec{k}_3|}, \end{aligned} \quad (\text{A1})$$

ϕ is the angle between the normals to the planes defined in the B_c rest frame by the $\bar{B}_s^0(J/\psi)\ell_1$ pair and the $\ell_2\pi^+$ pair. The ranges of the angular variables are $0 \leq \theta_{12} \leq \pi$, $0 \leq \theta_{34} \leq \pi$, and $-\pi \leq \phi \leq \pi$.

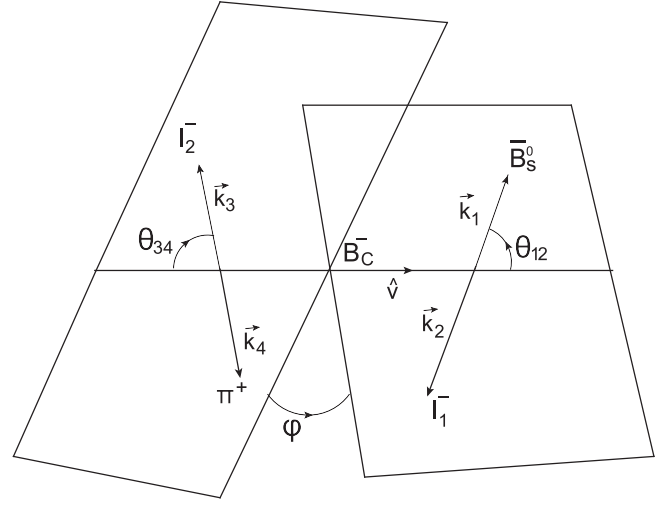


FIG. 12. Kinematics of four-body decays $B_c^- \rightarrow \bar{B}_s^0 \ell_1^- \ell_2^- \pi^+$ in the B_c rest frame.

To evaluate the decay rate for the 4-body LNV $B_c^- \rightarrow \bar{B}_s^0 \ell_1^- \ell_2^- \pi^+$ mode, the mod squared of the matrix element specified in Eq. (8) is expressed in terms of the dot products of the momenta of the final state particles as:

$$\begin{aligned} \sum |\mathcal{M}|^2 &= G_F^4 m_N^2 |V_{cs}|^2 |V_{ud}|^2 |V_{\ell_1 N} V_{\ell_2 N}|^2 f_\pi^2 \frac{\pi}{m_N \Gamma_N} \delta(p_N^2 - m_N^2) \\ &\times (8(F_+^2 + 2F_+ F_- + F_-^2)(m_4^2 m^2 (k_2 \cdot k_3) - 2m^2 (k_2 \cdot k_4)(k_3 \cdot k_4) + 4(k_2 \cdot p)(k_3 \cdot k_4)(k_4 \cdot p) \\ &- 2m_4^2 (k_2 \cdot p)(k_3 \cdot p)) + 8(F_+^2 - 2F_+ F_- + F_-^2)(m_4^2 m_1^2 (k_2 \cdot k_3) - 2m_1^2 (k_2 \cdot k_4)(k_3 \cdot k_4) \\ &+ 4(k_1 \cdot k_2)(k_3 \cdot k_4)(k_4 \cdot k_1) - 2m_4^2 (k_1 \cdot k_2)(k_1 \cdot k_3)) + 16(F_+^2 - F_-^2)(m_4^2 (k_2 \cdot k_3)(p \cdot k_1) \\ &- 2(k_2 \cdot k_4)(k_3 \cdot k_4)(p \cdot k_1) + 2(p \cdot k_2)(k_3 \cdot k_4)(k_1 \cdot k_4) - m_4^2 (p \cdot k_2)(k_1 \cdot k_3) + 2(k_1 \cdot k_2)(k_3 \cdot k_4) \\ &(p \cdot k_4) - m_4^2 (k_1 \cdot k_2)(p \cdot k_3))) + (k_2 \leftrightarrow k_3, m_2 \leftrightarrow m_3). \end{aligned} \quad (\text{A2})$$

Following are the explicit form of the four momenta of the final state particles $\bar{B}_s^0(k_1)$, $\ell_1^-(k_2)$, $\ell_2^-(k_3)$ and $\pi^+(k_4)$ in the B_c rest frame,

$$p = [m, 0, 0, 0];$$

$$\begin{aligned} k_1^\mu &= \left[\frac{\sqrt{M_{12}^2 + X^2}}{2M_{12}^2} (M_{12}^2 + m_1^2 - m_2^2) + \frac{X}{2} \cos(\theta_{12}) \lambda^{\frac{1}{2}} \left(1, \frac{m_1^2}{M_{12}^2}, \frac{m_2^2}{M_{12}^2} \right), \frac{1}{2} M_{12} \lambda^{\frac{1}{2}} \left(1, \frac{m_1^2}{M_{12}^2}, \frac{m_2^2}{M_{12}^2} \right) \sin(\theta_{12}), 0, \right. \\ &\left. \frac{1}{2} \sqrt{M_{12}^2 + X^2} \cos(\theta_{12}) \lambda^{\frac{1}{2}} \left(1, \frac{m_1^2}{M_{12}^2}, \frac{m_2^2}{M_{12}^2} \right) + \frac{X}{2M_{12}^2} (M_{12}^2 + m_1^2 - m_2^2) \right]; \end{aligned}$$

$$\begin{aligned} k_2^\mu &= \left[\frac{\sqrt{M_{12}^2 + X^2}}{2M_{12}^2} (M_{12}^2 + m_2^2 - m_1^2) - \frac{X}{2} \cos(\theta_{12}) \lambda^{\frac{1}{2}} \left(1, \frac{m_1^2}{M_{12}^2}, \frac{m_2^2}{M_{12}^2} \right), \right. \\ &\left. -\frac{1}{2} M_{12} \lambda^{\frac{1}{2}} \left(1, \frac{m_1^2}{M_{12}^2}, \frac{m_2^2}{M_{12}^2} \right) \sin(\theta_{12}), 0, -\frac{1}{2} \sqrt{M_{12}^2 + X^2} \cos(\theta_{12}) \lambda^{\frac{1}{2}} \left(1, \frac{m_1^2}{M_{12}^2}, \frac{m_2^2}{M_{12}^2} \right) + \frac{X}{2M_{12}^2} (M_{12}^2 + m_2^2 - m_1^2) \right]; \end{aligned}$$

$$\begin{aligned}
k_3^\mu &= \left[\frac{\sqrt{M_{34}^2 + X^2}}{2M_{34}^2} (M_{34}^2 + m_3^2 - m_4^2) - \frac{X}{2} \cos(\theta_{34}) \lambda^{\frac{1}{2}} \left(1, \frac{m_3^2}{M_{34}^2}, \frac{m_4^2}{M_{34}^2} \right), \frac{1}{2} M_{34} \lambda^{\frac{1}{2}} \left(1, \frac{m_3^2}{M_{34}^2}, \frac{m_4^2}{M_{34}^2} \right) \sin(\theta_{34}) \cos(\phi), \right. \\
&\quad \left. \frac{1}{2} M_{34} \lambda^{\frac{1}{2}} \left(1, \frac{m_3^2}{M_{34}^2}, \frac{m_4^2}{M_{34}^2} \right) \sin(\theta_{34}) \sin(\phi), \frac{1}{2} \sqrt{M_{34}^2 + X^2} \cos(\theta_{34}) \lambda^{\frac{1}{2}} \left(1, \frac{m_3^2}{M_{34}^2}, \frac{m_4^2}{M_{34}^2} \right) - \frac{X}{2M_{34}^2} (M_{34}^2 + m_3^2 - m_4^2) \right]; \\
k_4^\mu &= \left[\frac{\sqrt{M_{34}^2 + X^2}}{2M_{34}^2} (M_{34}^2 + m_4^2 - m_3^2) + \frac{X}{2} \cos(\theta_{34}) \lambda^{\frac{1}{2}} \left(1, \frac{m_3^2}{M_{34}^2}, \frac{m_4^2}{M_{34}^2} \right), \right. \\
&\quad - \frac{1}{2} M_{34} \lambda^{\frac{1}{2}} \left(1, \frac{m_3^2}{M_{34}^2}, \frac{m_4^2}{M_{34}^2} \right) \sin(\theta_{34}) \cos(\phi), - \frac{1}{2} M_{34} \lambda^{\frac{1}{2}} \left(1, \frac{m_3^2}{M_{34}^2}, \frac{m_4^2}{M_{34}^2} \right) \sin(\theta_{34}) \sin(\phi), \\
&\quad \left. - \frac{1}{2} \sqrt{M_{34}^2 + X^2} \cos(\theta_{34}) \lambda^{\frac{1}{2}} \left(1, \frac{m_3^2}{M_{34}^2}, \frac{m_4^2}{M_{34}^2} \right) - \frac{X}{2M_{34}^2} (M_{34}^2 + m_4^2 - m_3^2) \right]; \tag{A3}
\end{aligned}$$

where $X = \frac{1}{2m} \lambda^{\frac{1}{2}}(m^2, M_{12}^2, M_{34}^2)$. The results for $B_c^- \rightarrow J/\psi \ell_1^- \ell_2^- \pi^+$ are obtained in an analogous way, although they are a bit more complicated due to the additional form factors involved in the pseudoscalar to vector meson transition.

-
- [1] Y. Fukuda *et al.* (Super-Kamiokande Collaboration), Evidence for Oscillation of Atmospheric Neutrinos, *Phys. Rev. Lett.* **81**, 1562 (1998).
- [2] S. Fukuda *et al.* (Super-Kamiokande Collaboration), Constraints on Neutrino Oscillations using 1258 Days of Super-Kamiokande Solar Neutrino Data, *Phys. Rev. Lett.* **86**, 5656 (2001).
- [3] S. Fukuda *et al.* (Super-Kamiokande Collaboration), Determination of solar neutrino oscillation parameters using 1496 days of Super-Kamiokande I data, *Phys. Lett. B* **539**, 179 (2002).
- [4] Y. Ashie *et al.* (Super-Kamiokande Collaboration), Evidence for an Oscillatory Signature in Atmospheric Neutrino Oscillation, *Phys. Rev. Lett.* **93**, 101801 (2004).
- [5] B. T. Cleveland, T. Daily, R. Davis, Jr., J. R. Distel, K. Lande, C. K. Lee, P. S. Wildenhain, and J. Ullman, Measurement of the solar electron neutrino flux with the Homestake chlorine detector, *Astrophys. J.* **496**, 505 (1998).
- [6] W. Hampel *et al.* (GALLEX Collaboration), GALLEX solar neutrino observations: Results for GALLEX IV, *Phys. Lett. B* **447**, 127 (1999).
- [7] J. N. Abdurashitov *et al.* (SAGE Collaboration), Solar neutrino flux measurements by the Soviet-American Gallium Experiment (SAGE) for half the 22 year solar cycle, *Zh. Eksp. Teor. Fiz.* **122**, 211 (2002) [*J. Exp. Theor. Phys.* **95**, 181 (2002)].
- [8] Q. R. Ahmad *et al.* (SNO Collaboration), Measurement of the Rate of $\nu_e + d \rightarrow p + p + e^-$ Interactions Produced by 8B Solar Neutrinos at the Sudbury Neutrino Observatory, *Phys. Rev. Lett.* **87**, 071301 (2001).
- [9] Q. R. Ahmad *et al.* (SNO Collaboration), Direct Evidence for Neutrino Flavor Transformation from Neutral Current Interactions in the Sudbury Neutrino Observatory, *Phys. Rev. Lett.* **89**, 011301 (2002).
- [10] S. N. Ahmed *et al.* (SNO Collaboration), Measurement of the Total Active 8B Solar Neutrino Flux at the Sudbury Neutrino Observatory with Enhanced Neutral Current Sensitivity, *Phys. Rev. Lett.* **92**, 181301 (2004).
- [11] K. Eguchi *et al.* (KamLAND Collaboration), First Results from KamLAND: Evidence for Reactor Antineutrino Disappearance, *Phys. Rev. Lett.* **90**, 021802 (2003).
- [12] P. Minkowski, $\mu \rightarrow e\gamma$ at a rate of one out of 10^9 muon decays?, *Phys. Lett.* **67B**, 421 (1977).
- [13] T. Yanagida, in *Proceedings of the Workshop on Grand Unified Theory and Baryon Number of the Universe* (KEK, Japan, 1979).
- [14] M. Gell-Mann, P. Ramond, and R. Slansky, Report No. CALT-68-709; and in M. Gell-Mann, P. Ramond, and R. Slansky, in *Supergravity*, edited by D. Freedman *et al.* (North Holland, Amsterdam, 1979); S. L. Glashow, in *Quarks and Leptons, Cargese*, edited by M. Levy *et al.* (Plenum, New York, 1980), p. 707.
- [15] R. N. Mohapatra and G. Senjanovic, Neutrino Mass and Spontaneous Parity Violation, *Phys. Rev. Lett.* **44**, 912 (1980).
- [16] J. Schechter and J. W. F. Valle, Neutrino masses in $SU(2) \otimes U(1)$ theories, *Phys. Rev. D* **22**, 2227 (1980).
- [17] J. Schechter and J. W. F. Valle, Neutrino decay and spontaneous violation of lepton number, *Phys. Rev. D* **25**, 774 (1982).
- [18] I. Dorsner and P. Fileviez Perez, Upper bound on the mass of the Type III seesaw triplet in an $SU(5)$ model, *J. High Energy Phys.* **06** (2007) 029; B. Bajc, M. Nemevsek, and G. Senjanovic, Probing seesaw at LHC, *Phys. Rev. D* **76**, 055011 (2007).
- [19] A. de Gouvea, J. Jenkins, and N. Vasudevan, Neutrino phenomenology of very low-energy seesaw scenarios, *Phys. Rev. D* **75**, 013003 (2007); A. de Gouvea, GeV seesaw, accidentally small neutrino masses, and Higgs decays to neutrinos, arXiv:0706.1732.
- [20] C. Athanassopoulos *et al.* (LSND Collaboration), The liquid scintillator neutrino detector and LAMPF neutrino source,

- Nucl. Instrum. Methods Phys. Res., Sect. A **388**, 149 (1997).
- [21] J. M. Conrad, W. C. Louis, and M. H. Shaevitz, The LSND and MiniBooNE oscillation searches at high Δm^2 , *Annu. Rev. Nucl. Part. Sci.* **63**, 45 (2013).
- [22] A. A. Aguilar-Arevalo *et al.* (MiniBooNE Collaboration), A Search for Electron Neutrino Appearance at the $\Delta m^2 \sim 1 \text{ eV}^2$ Scale, *Phys. Rev. Lett.* **98**, 231801 (2007).
- [23] A. A. Aguilar-Arevalo *et al.* (MiniBooNE Collaboration), A Search for Electron Antineutrino Appearance at the $\Delta m^2 \sim 1 \text{ eV}^2$ Scale, *Phys. Rev. Lett.* **103**, 111801 (2009).
- [24] A. A. Aguilar-Arevalo *et al.* (MiniBooNE Collaboration), Improved Search for $\bar{\nu}_\mu \rightarrow \bar{\nu}_e$ Oscillations in the MiniBooNE Experiment, *Phys. Rev. Lett.* **110**, 161801 (2013).
- [25] Y. Abe *et al.* (Double Chooz Collaboration), Reactor electron antineutrino disappearance in the Double Chooz experiment, *Phys. Rev. D* **86**, 052008 (2012).
- [26] F. P. An *et al.* (Daya Bay Collaboration), Observation of Electron-Antineutrino Disappearance at Daya Bay, *Phys. Rev. Lett.* **108**, 171803 (2012).
- [27] J. K. Ahn *et al.* (RENO Collaboration), Observation of Reactor Electron Antineutrino Disappearance in the RENO Experiment, *Phys. Rev. Lett.* **108**, 191802 (2012).
- [28] S. Dodelson and L. M. Widrow, Sterile-Neutrinos as Dark Matter, *Phys. Rev. Lett.* **72**, 17 (1994).
- [29] X. D. Shi and G. M. Fuller, A New Dark Matter Candidate: Nonthermal Sterile Neutrinos, *Phys. Rev. Lett.* **82**, 2832 (1999); K. Abazajian, G. M. Fuller, and M. Patel, Sterile neutrino hot, warm, and cold dark matter, *Phys. Rev. D* **64**, 023501 (2001); K. N. Abazajian and G. M. Fuller, Bulk QCD thermodynamics and sterile neutrino dark matter, *Phys. Rev. D* **66**, 023526 (2002); G. M. Fuller, A. Kusenko, I. Mocioiu, and S. Pascoli, Pulsar kicks from a dark-matter sterile neutrino, *Phys. Rev. D* **68**, 103002 (2003); K. Abazajian, Production and evolution of perturbations of sterile neutrino dark matter, *Phys. Rev. D* **73**, 063506 (2006).
- [30] A. Kusenko, Sterile neutrinos: The dark side of the light fermions, *Phys. Rep.* **481**, 1 (2009); A. Kusenko, Detecting sterile dark matter in space, *Int. J. Mod. Phys. D* **16**, 2325 (2007); T. Asaka, M. Shaposhnikov, and A. Kusenko, Opening a new window for warm dark matter, *Phys. Lett. B* **638**, 401 (2006); P. L. Biermann and A. Kusenko, Relic keV Sterile Neutrinos and Reionization, *Phys. Rev. Lett.* **96**, 091301 (2006).
- [31] A. Boyarsky, O. Ruchayskiy, and M. Shaposhnikov, The role of sterile neutrinos in cosmology and astrophysics, *Annu. Rev. Nucl. Part. Sci.* **59**, 191 (2009); M. Shaposhnikov and I. Tkachev, The ν MSM, inflation, and dark matter, *Phys. Lett. B* **639**, 414 (2006).
- [32] H. J. de Vega and N. G. Sanchez, Model independent analysis of dark matter points to a particle mass at the keV scale, *Mon. Not. R. Astron. Soc.* **404**, 885 (2010); H. J. de Vega, P. Salucci, and N. G. Sanchez, The mass of the dark matter particle: From theory and galaxy observations, *New Astron.* **17**, 653 (2012); H. J. de Vega and N. G. Sanchez, Warm dark matter in the galaxies: theoretical and observational progresses. Highlights and conclusions of the challenge meudon workshop 2011, [arXiv:1109.3187](https://arxiv.org/abs/1109.3187); C. Destri, H. J. de Vega, and N. G. Sanchez, Fermionic warm dark matter produces galaxy cores in the observed scales because of quantum mechanics, *New Astron.* **22**, 39 (2013).
- [33] R. Adhikari *et al.*, A white paper on keV sterile neutrino dark matter, [arXiv:1602.04816](https://arxiv.org/abs/1602.04816).
- [34] F. S. Queiroz and K. Sinha, The poker face of the Majoron dark matter model: LUX to keV line, *Phys. Lett. B* **735**, 69 (2014).
- [35] R. E. Shrock, New tests for, and bounds on, neutrino masses and lepton mixing, *Phys. Lett.* **96B**, 159 (1980).
- [36] A. Atre, T. Han, S. Pascoli, and B. Zhang, The search for heavy Majorana neutrinos, *J. High Energy Phys.* **05** (2009) 030.
- [37] G. Cvetic, C. Dib, S. K. Kang, and C. S. Kim, Probing Majorana neutrinos in rare K and D, D_s , B , B_c meson decays, *Phys. Rev. D* **82**, 053010 (2010); G. Cvetic, C. Dib, and C. S. Kim, Probing Majorana neutrinos in rare $\pi^+ \rightarrow e^+ e^+ \mu^- \nu$ decays, *J. High Energy Phys.* **06** (2012) 149.
- [38] J. C. Helo, S. Kovalenko, and I. Schmidt, Sterile neutrinos in lepton number and lepton flavor violating decays, *Nucl. Phys.* **B853**, 80 (2011).
- [39] Q. He *et al.* (CLEO Collaboration), Search for Rare and Forbidden Decays $D^+ \rightarrow h^\pm e^\mp e^+$, *Phys. Rev. Lett.* **95**, 221802 (2005).
- [40] Y. Kubota *et al.* (CLEO Collaboration), The CLEO-II detector, *Nucl. Instrum. Methods Phys. Res., Sect. A* **320**, 66 (1992).
- [41] P. Rubin *et al.* (CLEO Collaboration), Search for rare and forbidden decays of charm and charmed-strange mesons to final states $h^+ - e^- + e^+$, *Phys. Rev. D* **82**, 092007 (2010).
- [42] J. M. Link *et al.* (FOCUS Collaboration), Search for rare and forbidden three body dimuon decays of the charmed mesons D^+ and D_s^+ , *Phys. Lett. B* **572**, 21 (2003).
- [43] J. P. Lees *et al.* (BABAR Collaboration), Searches for rare or forbidden semileptonic charm decays, *Phys. Rev. D* **84**, 072006 (2011).
- [44] R. Aaij *et al.* (LHCb Collaboration), Search for the Lepton Number Violating Decays $B^+ \rightarrow \pi^- \mu^+ \mu^+$ and $B^+ \rightarrow K^- \mu^+ \mu^+$, *Phys. Rev. Lett.* **108**, 101601 (2012); M. Patel, in *Workshop on Flavor and the Fourth Family, IPPP Durham, 2011*, <http://conference.ippp.dur.ac.uk/event/316/> program.
- [45] M. Dittmar, A. Santamaria, M. C. Gonzalez-Garcia, and J. W. F. Valle, Production mechanisms and signatures of isosinglet neutral heavy leptons in Z^0 decays, *Nucl. Phys.* **B332**, 1 (1990).
- [46] F. del Aguila, J. A. Aguilar-Saavedra, and R. Pittau, Neutrino physics at large colliders, *J. Phys. Conf. Ser.* **53**, 506 (2006).
- [47] W. Buchmuller and C. Greub, Heavy Majorana neutrinos in electron—positron and electron—proton collisions, *Nucl. Phys.* **B363**, 345 (1991).
- [48] F. M. L. Almeida, Jr., Y. D. A. Coutinho, J. A. Martins Simoes, and M. A. B. do Vale, Neutral heavy lepton production at next high-energy $e^+ e^-$ linear colliders, *Phys. Rev. D* **63**, 075005 (2001).
- [49] F. F. Deppisch, P. S. Bhupal Dev, and A. Pilaftsis, Neutrinos and collider physics, *New J. Phys.* **17**, 075019 (2015).
- [50] S. Banerjee, P. S. B. Dev, A. Ibarra, T. Mandal, and M. Mitra, Prospects of heavy neutrino searches at future lepton colliders, *Phys. Rev. D* **92**, 075002 (2015).

- [51] S. Bray, J. S. Lee, and A. Pilaftsis, Heavy Majorana neutrino production at $e^- \gamma$ colliders, *Phys. Lett. B* **628**, 250 (2005).
- [52] P. S. B. Dev, A. Pilaftsis, and U. k. Yang, New Production Mechanism for Heavy Neutrinos at the LHC, *Phys. Rev. Lett.* **112**, 081801 (2014).
- [53] A. Das, P. S. Bhupal Dev, and N. Okada, Direct bounds on electroweak scale pseudo-Dirac neutrinos from $\sqrt{s} = 8$ TeV LHC data, *Phys. Lett. B* **735**, 364 (2014).
- [54] W.-Y. Keung and G. Senjanovic, Majorana Neutrinos and the Production of the Right-Handed Charged Gauge Boson, *Phys. Rev. Lett.* **50**, 1427 (1983); T. H. Ho, C. R. Ching, and Z. J. Tao, Production of right-handed gauge boson and heavy Majorana neutrino in SSC, *Phys. Rev. D* **42**, 2265 (1990); D. A. Dicus, D. D. Karatas, and P. Roy, Lepton nonconservation at supercollider energies, *Phys. Rev. D* **44**, 2033 (1991); A. Datta, M. Guchait, and D. P. Roy, Prospect of heavy right-handed neutrino search at SSC / CERN LHC energies, *Phys. Rev. D* **47**, 961 (1993); A. Ferrari, J. Collot, M. L. Andrieux, B. Belhorma, P. de Saintignon, J. Y. Hostachy, P. Martin, and M. Wielers, Sensitivity study for new gauge bosons and right-handed Majorana neutrinos in pp collisions at $s = 14$ TeV, *Phys. Rev. D* **62**, 013001 (2000).
- [55] A. Ali, A. V. Borisov, and N. B. Zamorin, Majorana neutrinos and same sign dilepton production at LHC and in rare meson decays, *Eur. Phys. J. C* **21**, 123 (2001).
- [56] F. M. L. Almeida, Jr., Y. D. A. Coutinho, J. A. Martins Simoes, and M. A. B. do Vale, On a signature for heavy Majorana neutrinos in hadronic collisions, *Phys. Rev. D* **62**, 075004 (2000).
- [57] T. Han and B. Zhang, Signatures for Majorana Neutrinos at Hadron Colliders, *Phys. Rev. Lett.* **97**, 171804 (2006).
- [58] T. G. Rizzo, Inverse neutrinoless double beta decay, *Phys. Lett.* **116B**, 23 (1982); C. A. Heusch and P. Minkowski, Lepton flavor violation induced by heavy Majorana neutrinos, *Nucl. Phys.* **B416**, 3 (1994).
- [59] S. Bar-Shalom, N. G. Deshpande, G. Eilam, J. Jiang, and A. Soni, Majorana neutrinos and lepton-number-violating signals in top-quark and W-boson rare decays, *Phys. Lett. B* **643**, 342 (2006).
- [60] N. Quintero, G. Lopez Castro, and D. Delepine, Lepton number violation in top quark and neutral B meson decays, *Phys. Rev. D* **84**, 096011 (2011); **86**, 079905(E) (2012).
- [61] R. Aaij *et al.* (LHCb Collaboration), Observation of the Decay $B_c^+ \rightarrow B_s^0 \pi^+$, *Phys. Rev. Lett.* **111**, 181801 (2013).
- [62] G. Aad *et al.* (ATLAS Collaboration), Study of the $B_c^+ \rightarrow J/\psi D_s^+$ and $B_c^+ \rightarrow J/\psi D_s^{*+}$ decays with the ATLAS detector, *Eur. Phys. J. C* **76**, 4 (2016).
- [63] V. Khachatryan *et al.* (CMS Collaboration), Measurement of the ratio of the production cross sections times branching fractions of $B_c^\pm \rightarrow J/\psi \pi^\pm$ and $B^\pm \rightarrow J/\psi K^\pm$ and $\mathcal{B}(B_c^\pm \rightarrow J/\psi \pi^\pm \pi^\pm \pi^\mp) / \mathcal{B}(B_c^\pm \rightarrow J/\psi \pi^\pm)$ in pp collisions at $\sqrt{s} = 7$ TeV, *J. High Energy Phys.* **01** (2015) 063.
- [64] R. Aaij *et al.* (LHCb Collaboration), Measurements of B_c^+ Production and Mass with the $B_c^+ \rightarrow J/\psi \pi^+$ Decay, *Phys. Rev. Lett.* **109**, 232001 (2012); N. Brambilla *et al.* (Quarkonium Working Group Collaboration), Heavy quarkonium physics, [arXiv:hep-ph/0412158](https://arxiv.org/abs/hep-ph/0412158).
- [65] V. V. Kiselev, A. E. Kovalsky, and A. K. Likhoded, B_c decays and lifetime in QCD sum rules, *Nucl. Phys.* **B585**, 353 (2000); V. V. Kiselev, Exclusive decays and lifetime of B_c meson in QCD sum rules, [arXiv:hep-ph/0211021](https://arxiv.org/abs/hep-ph/0211021).
- [66] K. A. Olive *et al.* (Particle Data Group Collaboration), Review of particle physics, *Chin. Phys. C* **38**, 090001 (2014).
- [67] M. C. Gonzalez-Garcia, M. Maltoni, and T. Schwetz, Global analyses of neutrino oscillation experiments, *Nucl. Phys.* **B908**, 199 (2016).
- [68] S. Parke and M. Ross-Lonergan, Unitarity and the three flavour neutrino mixing matrix, *Phys. Rev. D* **93**, 113009 (2016).
- [69] S. Bergmann and A. Kagan, Z-induced FCNCs and their effects on neutrino oscillations, *Nucl. Phys.* **B538**, 368 (1999).
- [70] F. del Aguila, J. de Blas, and M. Perez-Victoria, Effects of new leptons in electroweak precision data, *Phys. Rev. D* **78**, 013010 (2008).
- [71] M. Drewes and B. Garbrecht, Experimental and cosmological constraints on heavy neutrinos, [arXiv:1502.00477](https://arxiv.org/abs/1502.00477).
- [72] G. Lopez Castro and N. Quintero, Lepton number violating four-body tau lepton decays, *Phys. Rev. D* **85**, 076006 (2012); **86**, 079904(E) (2012).
- [73] H. Yuan, T. Wang, G. L. Wang, W. L. Ju, and J. M. Zhang, Lepton-number violating four-body decays of heavy mesons, *J. High Energy Phys.* **08** (2013) 066.
- [74] H. R. Dong, F. Feng, and H. B. Li, Lepton number violation in D meson decay, *Chin. Phys. C* **39**, 013101 (2015).
- [75] G. Lopez Castro and N. Quintero, Lepton number violation in tau lepton decays, *Nucl. Phys. B, Proc. Suppl.* **253–255**, 12 (2014).
- [76] R. Aaij *et al.* (LHCb Collaboration), Searches for Majorana neutrinos in B^- decays, *Phys. Rev. D* **85**, 112004 (2012).
- [77] C. H. Chang, C. Driouichi, P. Eerola, and X. G. Wu, BCVEGPY: An event generator for hadronic production of the B_c meson, *Comput. Phys. Commun.* **159**, 192 (2004).
- [78] Our crude estimate is based on private communication with Vanya Belyaev from the LHCb collaboration.
- [79] R. Aaij *et al.* (LHCb Collaboration), Measurement of B_c^+ Production in Proton-Proton Collisions at $\sqrt{s} = 8$ TeV, *Phys. Rev. Lett.* **114**, 132001 (2015).
- [80] A. de Gouvêa and A. Kobach, Global constraints on a heavy neutrino, *Phys. Rev. D* **93**, 033005 (2016).
- [81] P. Vilain *et al.* (CHARM II Collaboration), Search for heavy isosinglet neutrinos, *Phys. Lett. B* **343**, 453 (1995); **351**, 387 (1995).
- [82] J. Orloff, A. N. Rozanov, and C. Santoni, Limits on the mixing of tau neutrino to heavy neutrinos, *Phys. Lett. B* **550**, 8 (2002).
- [83] P. Astier *et al.* (NOMAD Collaboration), Search for heavy neutrinos mixing with tau neutrinos, *Phys. Lett. B* **506**, 27 (2001).
- [84] P. Abreu *et al.* (DELPHI Collaboration), Search for neutral heavy leptons produced in Z decays, *Z. Phys. C* **74**, 57 (1997); **75**, 580(E) (1997).
- [85] A. Kobach and S. Dobbs, Heavy neutrinos and the kinematics of tau decays, *Phys. Rev. D* **91**, 053006 (2015).